

FISSION DYNAMICS STUDIES OF NEAR SUPER-HEAVY COMPOUND NUCLEUS $^{256}\text{Rf}^*$

MEENU THAKUR^a, B.R. BEHERA^a, RUCHI MAHAJAN^a, N. SANEESH^b
GURPREET KAUR^a, PRIYA SHARMA^a, R. DUBEY^b, KUSHAL KAPOOR^a
A. YADAV^b, NEERAJ KUMAR^c, S. KUMAR^d, KAVITA RANI^a
P. SUGATHAN^b, A. JHINGAN^b, A. CHATTERJEE^b, M.B. CHATTERJEE^b
S. MANDAL^c, A. SAXENA^e, SANTANU PAL^{f,†}, S. KAILAS^e

^aDepartment of Physics, Panjab University, Chandigarh-160014, India

^bInter University Accelerator Center, New Delhi-110067, India

^cDepartment of Physics and Astrophysics, University of Delhi-110007, India

^dDepartment of Nuclear Physics, Andhra University-530003, India

^eNuclear Physics Division, Bhabha Atomic Research Centre
Mumbai-400085, India

^fCS-6/1, Golf Green, Kolkata-700095, India

(Received January 10, 2018)

To understand the fission dynamics of ^{256}Rf , we performed neutron multiplicity measurements for the reaction $^{48}\text{Ti}+^{208}\text{Pb}$ at an excitation energy of 57.4 MeV. The results confirmed the presence of quasi-fission processes in this system. The experimental neutron multiplicities have also been compared with the theoretical predictions from statistical model calculations. From this comparison, the value of reduced dissipation strength for the ^{256}Rf nucleus is found to be $(7.6 \pm 0.7) \times 10^{21} \text{ s}^{-1}$ and a fission delay time of $(39.6_{-4.1}^{+4.6}) \times 10^{-21} \text{ s}$ has been estimated.

DOI:10.5506/APhysPolB.49.631

1. Introduction

Synthesis of super-heavy elements (SHE) using long experiments involving the fusion of two massive nuclei is an area of intense research in nuclear physics. The planning of these expensive experiments requires a precise knowledge of fission observables such as mass and total kinetic energy of the fission fragments produced in the reaction. The reaction mechanism

* Presented at the XXXV Mazurian Lakes Conference on Physics, Piaski, Poland, September 3–9, 2017.

† Formerly with VECC, Kolkata, India.

toward heavy and super-heavy nuclei is dominated by the fusion–fission (FF) and quasi-fission (QF) processes [1]. Studies of the properties of FF and QF processes act as a baseline to understand the reaction dynamics and evolution of several degrees of freedom in the formation of the compound nucleus (CN). Numerous measurements *viz.* fission fragment angular distribution, mass distribution, and mass–energy and mass–angle correlations are used to distinguish between FF, QF and deep inelastic collision components [2, 3]. However, it is observed that mass distribution, energy distribution, mass–energy and mass–angle correlations are not sufficient to disentangle the above-mentioned components in the fission path of a heavy element, as the mass-symmetric region may be populated both by FF and QF processes. It is shown by dynamical calculations applying the Langevin equations to study the time evolution of nuclear shape that the FF and QF processes have different reaction times from the contact of the colliding partners to the scission point [4]. The different reaction timescales imply that each reaction process is associated with a different pre-scission neutron multiplicity [5]. With this motivation, we have studied the mass distribution, mass–energy and mass–angle correlations, average neutron multiplicity, mass-gated and energy-gated neutron multiplicity, and neutron angular distribution for the $^{48}\text{Ti}+^{208}\text{Pb}$ reaction populating the near super-heavy nucleus ^{256}Rf at an excitation energy of 57.4 MeV, well above the Coulomb barrier. In the present paper, we are reporting the results for average and fission fragment mass-gated neutron multiplicity measurements performed to study the fission dynamics of ^{256}Rf .

2. Results and discussion

The details of the experimental setup and the data analysis for the extraction of neutron multiplicity are available in Ref. [6]. To reduce the angular uncertainty arising from the large active area of multi-wire proportional counters (MWPC), they are sliced into four pieces of the same size 3.1 cm \times 5.1 cm. The angular coverage of each of these slices is $\pm 3.5^\circ$ in polar angle (θ) and $\pm 5.8^\circ$ in azimuthal angle (ϕ). To deduce the average neutron multiplicities, neutron TOF spectra are further gated with timing correlation of MWPCs represented as the area enclosed within the black solid line shown in Fig. 1. In order to extract neutron multiplicities, the recorded TOF spectra are used to obtain the neutron energy spectra following the procedure described in Ref. [6]. The neutron energy spectra thus obtained are then corrected for efficiency of the neutron detectors calculated using the statistical model code FLUKA at a threshold of 120 KeVee. The neutron energy spectra obtained experimentally may have contributions from three sources: CN (pre-scission), fission fragment (FF1) (post-scission), and the complementary fission fragment (FF2) (post-scission).

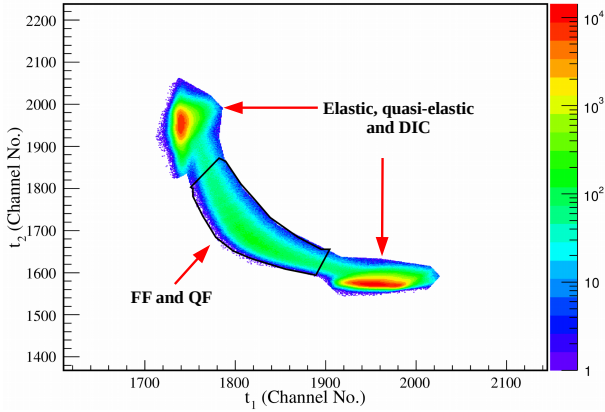


Fig. 1. Timing correlation between the two MWPCs for the $^{48}\text{Ti}+^{208}\text{Pb}$ reaction.

The pre- and post-scission components of neutron multiplicities are thus derived by carrying out moving source fits to the observed neutron energy spectra at various angles using the Watt expression [7]. The neutron multiplicity and temperature are assumed to be the same for both fission fragments ($M_n^{\text{FF1}} = M_n^{\text{FF2}}$ and $T_{\text{FF1}} = T_{\text{FF2}} = T_{\text{post}}$) and the total neutron multiplicity can be given as: $M_n^{\text{total}} = M_n^{\text{pre}} + M_n^{\text{post}}$, where M_n^{pre} is the pre-scission neutron multiplicity and $M_n^{\text{post}} = M_n^{\text{FF1}} + M_n^{\text{FF2}}$ is the total post-scission neutron multiplicity. Energy spectra of all the neutron detectors are fitted simultaneously keeping M_n^{pre} , M_n^{FF1} , T_{pre} and T_{post} as free parameters. The simultaneous fitting is obtained by the chi-square minimization technique. The obtained values of average M_n^{pre} , M_n^{post} , and M_n^{total} , resulting from the simultaneous fit of 388 neutron energy spectra from neutron detectors placed at different angles, are 1.68 ± 0.10 , 6.14 ± 0.10 and 7.82 ± 0.14 , respectively. Figure 2 shows the fits to the double-differential neutron multiplicity spectra along with the contributions from different sources at various angles for the $^{48}\text{Ti}+^{208}\text{Pb}$ system at $E_{\text{lab}} = 273.1$ MeV. From this figure, it is clear that the contribution from different neutron sources varies significantly with the correlation angle between the fission fragment and the neutron detector. A substantial presence of QF processes is indicated in the $^{48}\text{Ti}+^{208}\text{Pb}$ system by the results of the fission fragment mass distribution analysis [8]. For consistency, the variation of neutron multiplicity with fission fragment mass was investigated in order to separate out the QF and FF contributions [9]. It was observed that M_n^{total} increases from 0.44 ± 0.02 to 8.25 ± 0.10 when going from projectile-like fragments (PLF) to a symmetric mass split. In the same manner, M_n^{pre} was also found to increase from PLF ($M_n^{\text{pre}} = 0.15 \pm 0.01$) to a symmetric mass split ($M_n^{\text{pre}} = 2.23 \pm 0.07$), which could be explained on the basis of the expected increase in the available ex-

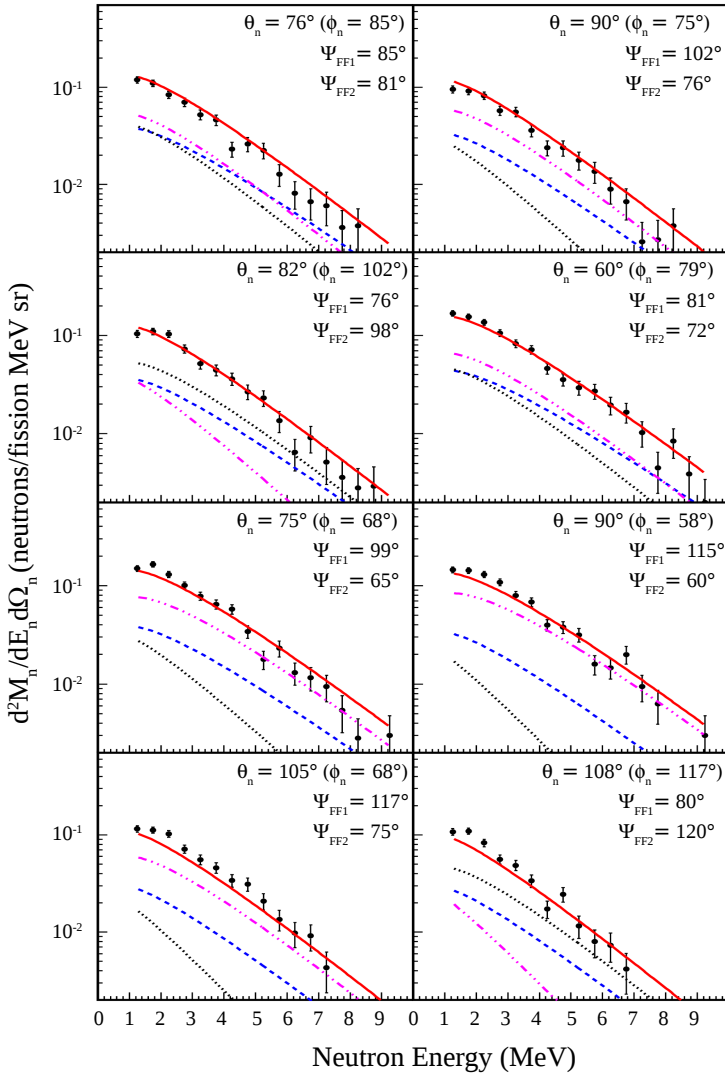


Fig. 2. Fits to the double-differential neutron multiplicity spectra (solid black circles) along with the contributions from pre-scission (dashed blue line) and post-scission components (dotted/black and dash-dotted/pink lines correspond to symmetric mass fragments detected in the MWPCs located at forward and backward angles, respectively) from both the fission fragments corresponding to the neutron detectors placed at different angles, for the $^{48}\text{Ti}+^{208}\text{Pb}$ system at $E_{\text{lab}} = 273.1$ MeV. The solid/red line corresponds to the total contribution.

citation energy with this transition. The enhancement in M_n^{pre} when going from the asymmetric ($M_n^{\text{pre}} = 1.66 \pm 0.07$) to the symmetric mass region ($M_n^{\text{pre}} = 2.23 \pm 0.07$) may be due to the different timescales of the FF and QF processes. The observed neutron multiplicities for the three mass splits are compatible with the recent results reported for the nearby $^{50}\text{Ti}+^{208}\text{Pb}$ system [10].

The experimentally deduced average M_n^{pre} and M_n^{post} are further compared with the statistical model predictions for the $^{48}\text{Ti}+^{208}\text{Pb}$ system [11]. The fission barrier in the present calculations is obtained by including shell corrections to the liquid-drop nuclear mass [12]. Shell effects are also included in the nuclear level density which is used to calculate various decay widths of the CN. To this end, we use the level density parameter from the work of Ignatyuk *et al.* [13]. In the statistical model of CN decay, the fission occurs when the CN crosses the saddle point. The number of neutrons emitted by the CN during its progression from the saddle to the scission configuration contributes to M_n^{pre} and is calculated using the saddle-to-scission transit time interval (τ_{ss}°) [14].

The value of pre-scission neutron multiplicity ($M_n^{\text{pre}} = 0.25$) for the reaction $^{48}\text{Ti}+^{208}\text{Pb}$ at an excitation energy of 57.4 MeV, calculated using the Bohr–Wheeler fission width, is significantly lower than the experimentally measured value. This immediately suggests that a fission hindrance is required to reproduce the pre-scission neutron multiplicity. In a dissipative dynamical model of fission, a reduction in fission width can be obtained from the Kramers modified fission width [15] following:

$$\Gamma_{\text{K}} = \Gamma_{\text{BW}} \left[\sqrt{1 + \left(\frac{\beta}{2\omega_{\text{s}}} \right)^2} - \frac{\beta}{2\omega_{\text{s}}} \right], \quad (1)$$

where Γ_{BW} is the Bohr–Wheeler fission width, β is the reduced dissipation coefficient and ω_{s} is the frequency of a harmonic oscillator potential at the saddle configuration. Introduction of dissipation also changes the saddle-to-scission time interval [14].

Statistical model calculations were performed for the $^{48}\text{Ti}+^{208}\text{Pb}$, $^{28}\text{Si}+^{232}\text{Th}$ and $^{19}\text{F}+^{232}\text{Th}$ reactions for different values of β . The variation of M_n^{pre} with β is shown in Fig. 3(a). This figure shows that M_n^{pre} decreases with the increase in projectile mass (from ^{19}F to ^{48}Ti), which may be an effect of lowering of fission barrier at higher compound nucleus spin related to the use of heavier projectiles.

We found that the experimentally measured value of M_n^{pre} (1.68 ± 0.10) for $^{48}\text{Ti}+^{208}\text{Pb}$ system can be reproduced by β value of $(7.6 \pm 0.7) \times 10^{21} \text{ s}^{-1}$. The strength of the dissipation thus found is close to the value reported for the CN ^{260}Rf populated using the $^{20}\text{Ne}+^{240}\text{Pu}$ reaction [16]. In order to get

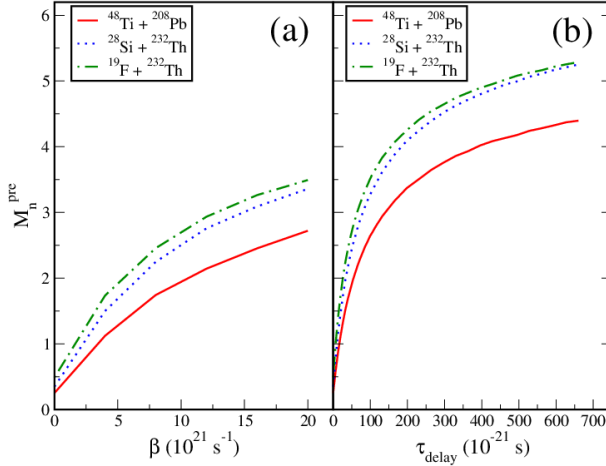


Fig. 3. Variation of the pre-scission neutron multiplicity (M_n^{pre}) with (a) the reduced dissipation coefficient (β), and (b) delay time (τ_{delay}) for the $^{48}\text{Ti} + ^{208}\text{Pb}$, $^{28}\text{Si} + ^{232}\text{Th}$ and $^{19}\text{F} + ^{232}\text{Th}$ reactions at an excitation energy of 57.4 MeV.

a direct estimate of the time delay required for the emission of the experimentally observed number of pre-scission neutrons, we performed another set of calculations where a delay time (τ_{delay}) was introduced in the saddle-to-scission stage of fission. The total saddle-to-scission transition time is then given as ($\tau_{\text{ss}}^o + \tau_{\text{delay}}$). The variation of M_n^{pre} with τ_{delay} for the three systems is shown in Fig. 3 (b), indicating a lower value of M_n^{pre} for the $^{48}\text{Ti} + ^{208}\text{Pb}$ system as compared to other two systems. This is an artifact of the significant contributions from QF processes in the $^{48}\text{Ti} + ^{208}\text{Pb}$ reaction due to its high entrance-channel mass asymmetry or charge product ($Z_1 Z_2$; where Z_1 and Z_2 are the atomic numbers of projectile and target, respectively). A fission delay of $(39.6^{+4.6}_{-4.1}) \times 10^{-21} \text{ s}$ has been found to correspond to the experimentally observed value of M_n^{pre} equal to 1.68 ± 0.10 for the $^{48}\text{Ti} + ^{208}\text{Pb}$ system. This shorter delay time indicates the presence of QF processes in this heavy system. For the $^{19}\text{F} + ^{232}\text{Th}$ reaction, we have also reproduced the available experimental values of M_n^{pre} from Ref. [17] in E^* range of 54–90 MeV, by varying τ_{delay} . A τ_{delay} value of $33 \times 10^{-21} \text{ s}$ was required to reproduce the experimental data. Figure 4 shows M_n^{pre} at different E^* values for the fitted value of τ_{delay} . This value is in a good agreement with that reported in Ref. [17] and is also comparable with what we obtained for the $^{48}\text{Ti} + ^{208}\text{Pb}$ system. Theoretical calculations corresponding to the symmetric and asymmetric mass cuts are in progress.

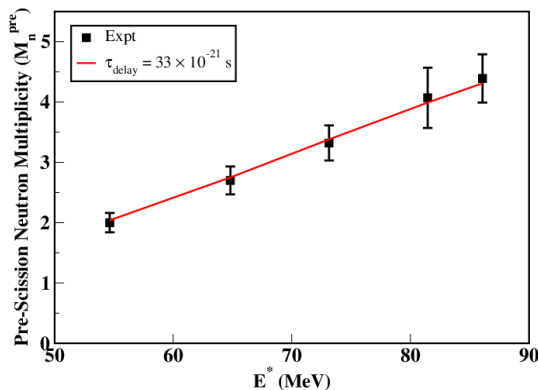


Fig. 4. Variation of M_n^{pre} with E^* for the fitted value of $\tau_{\text{delay}} = 33 \times 10^{-21}$ s in the $^{19}\text{F} + ^{232}\text{Th}$ reaction.

REFERENCES

- [1] M.G. Itkis *et al.*, *Nucl. Phys. A* **734**, 136 (2004).
- [2] D.J. Hinde *et al.*, *EPJ Web Conf.* **17**, 04001 (2011).
- [3] M.G. Itkis *et al.*, *EPJ Web Conf.* **17**, 12002 (2011).
- [4] D. Jacquet, M. Morjean, *Prog. Part. Nucl. Phys.* **63**, 155 (2009).
- [5] Y. Aritomo *et al.*, *Nucl. Phys. A* **759**, 342 (2005).
- [6] M. Thakur *et al.*, *Proceedings of the DAE-BRNS Symp. on Nucl. Phys.* **60**, 358 (2015).
- [7] D. Hilscher *et al.*, *Phys. Rev. C* **20**, 576 (1979).
- [8] M. Thakur *et al.*, *Eur. Phys. J. A* **53**, 133 (2017).
- [9] M. Thakur *et al.*, *Proceedings of the DAE-BRNS Symp. on Nucl. Phys.* **61**, 388 (2016).
- [10] S. Appannababu *et al.*, *Phys. Rev. C* **94**, 044618 (2016).
- [11] J. Sadhukhan, S. Pal, *Phys. Rev. C* **78**, 011603(R) (2008) [*Erratum ibid.* **79**, 019901 (2009)].
- [12] K. Mahata, S. Kailas, S.S. Kapoor, *Phys. Rev. C* **92**, 034602 (2015).
- [13] A.V. Ignatyuk, G.M. Smirenkin, A. Tishin, *Sov. J. Nucl. Phys.* **21**, 255 (1975).
- [14] H. Hofmann, J.R. Nix, *Phys. Lett. B* **122**, 117 (1983).
- [15] H.A. Kramers, *Physica (Amsterdam)* **7**, 284 (1940).
- [16] Meenu Thakur *et al.*, *Proceedings of the DAE Symp. on Nucl. Phys.* **58**, 546 (2013).
- [17] J.O. Newton *et al.*, *Nucl. Phys. A* **483**, 126 (1988).